Monte Carlo Simulation of the Dynamics and Quasielastic Scattering in Many-Chain Polymer Systems

Antonio López Rodriguez, Antonio Rey, and Juan J. Freire*

Departamento de Quimica Fisica, Facultad de Ciencias Quimicas, Universidad Complutense, 28040 Madrid, Spain

Received December 10, 1991; Revised Manuscript Received March 2, 1992

ABSTRACT: A dynamic Monte Carlo algorithm has been employed to simulate different dynamic properties for dilute and nondilute polymer systems, mainly in the good solvent regime (with excluded volume conditions). The results for translational diffusion coefficients, relaxation times of the end-to-end vector and the internal Rouse coordinates, the dynamic form factor of individual chains, and the dynamic collective scattering function of the systems are analyzed. The variations of these properties with chain length and concentration are discussed and compared with previous simulation results, theoretical predictions, or experimental behaviors.

Introduction

Monte Carlo (MC) techniques have been widely used to simulate the dynamic properties of polymer chains.[1-5] Simultaneously, the theoretical bases of dynamic MC methods have been discussed by several authors.[6,7] Although current MC algorithms cannot describe some important features of polymer solutions as the effects of hydrodynamic interactions (HI) between polymer units,[8,9] their description of polymer dynamics is compatible with the simple Rouse model for dilute solution.[10] Their application is, however, more interesting in the case of many-chain nondilute systems where HI are somehow canceled out. Moreover, the MC methods for lattice models are specially efficient to explore these systems, which, on the other hand, are very difficult to study through purely dynamic methods (Brownian dynamics or molecular dynamics), given their great complexity.

Some properties have been investigated thoroughly by means of MC dynamic simulations in the recent past. Thus, results for the translational diffusion coefficient and the relaxation times of the end-to-end vector and different internal Rouse coordinates have been reported for both the dilute and the nondilute regimes,[2-5] and the dependence of these properties with the chain length has been analyzed. A good reproduction of the Rouse dynamics has been obtained in the dilute systems, after some technical problems related with the type of motions included in the algorithm[1,11] were properly solved. Calculations for nondilute systems have been mainly aimed to test the validity of the popular reptation theory. The results obtained up to the present are not, however, conclusive on this crucial and controversial point.[7,12]

Radiation scattering is one of the most direct experimental techniques to explore the dynamics of polymer systems.[13] The interpretation of results can be easily performed for dilute systems, since appropriate theories have been established to link these results with molecular motions.[14] Nevertheless, nondilute systems still constitute a theoretical[9] and experimental[15] challenge, because the experiments monitor fluctuations of density which correspond to cooperative motions in local regions of the system, and these motions may involve several chains.

In the present work, we use a dynamic MC method (with slight differences with respect to those previously employed) to calculate different properties of dilute and nondilute chains in a simple cubic lattice. We consider the condition of single site occupation by polymer units in most of our calculations. This condition introduces an excluded volume (EV) effect and, therefore, is adequate to describe polymers in the good solvent regime. Some calculations in the dilute regime are also performed, allowing multiple occupation by polymer units which are not neighbors along a chain contour. This random walk model (RW) corresponds to ideal chains without long-range interactions.

We obtain results for diffusion coefficients and relaxation times whose variation with chain length and concentration are compared to theoretical predictions,[9] and also with those previously obtained with other MC algorithms.[2-5] Moreover, we obtain dynamic scattering functions which correspond to the radiation intensity scattered by the systems. The simulation data for these functions are properly analyzed in terms of sums of exponential contributions. In the dilute case, and according to theories based in the Rouse model,[14] this analysis should provide an alternative estimation of diffusion coefficients and, on same occasions, of relaxation times, which may provide further indication of the ability of MC methods to reproduce the chain dynamics. For the nondilute systems, the lack of a detailed theoretical description of cooperative motions makes the analysis of simulation results especially interesting.

Methods

Our MC method considers one or many (n) polymer chains, each one of them composed of N units which are placed in the sites of a simple cubic lattice. The lattice size is fixed by the length of a cube, L, accordingly to previously established criteria.[12] Periodic boundary conditions are employed in the customary way. The empty sites (or voids) are assumed to be filled by solvent occupying the same volume than the polymer units. The fraction of polymer sites or polymer volume fraction, Φ, is fixed for the system. In most simulations only 1 polymer unit per site is allowed. This way, we introduce an EV effect, consistent with good thermodinamic solvent conditions. Also, some simulations in the dilute regime (one chain in the lattice) are performed with the RW model, which allow for multiple occupation of sites by non-neighboring polymer units, consistent with ideal representations of chains without long-range interactions.

The configurations change according to several types of motions which are considered representations of the real polymer dynamics;[1-5] thus, we introduce the usual end motions, where a terminal bond is changed to a perpendicular direction. We also consider inner local motions as bents and crankshafts, involving two or three bonds, respectively. All of these motions have been also con-

0024-9297/92/2225-3266$03.00/0

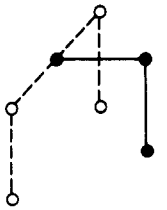

Figure 1. Two-bond end (or broken crankshaft) motion.

sidered in previous simulations.[1-5,11] We also introduce a two-bond end motion or broken crankshaft. In this motion, two terminal and perpendicular bonds suffer a 90° rotation (Figure 1). The motion permits an increase in the number of new bond vectors generated through the simulation and is consistent with the presence of inner crankshaft motions (since the usual one-bond end motions can be considered as broken bents).

In order to perform a configurational change, we randomly select one of the different polymer units in the system. If it corresponds to a terminal unit, one of the usual end motions is attempted. If it is adjacent to a terminal unit, and the bonds attached to it are perpendicular, we choose randomly whether a normal bent or a two-bond end motion is attempted. Finally, for inner units attached to perpendicular bonds, a bent or a crankshaft motion can be tried. Of course, if the single occupation condition has been established, it is checked after any of these changes, and the old configuration is counted again when this condition cannot be satisfied.

We define the unit time as the number of simulation steps (or attempted configurational changes) needed to give a chance to move to all the different polymer units in the system. Then, the time that corresponds to a configuration generated after k steps will be $t_k = k/(nN)$. The length unit corresponds to the distance b between nearest neighbor lattice sites.

The procedures to obtain an initial configuration are similar to those employed in our previous studies of equilibrium properties with the same lattice model.[16,17] A thermal equilibration of (1-10) × 10^6 configuration steps (depending on the chain length and concentration) is performed before starting the dynamical simulation. This equilibration is reached with the more efficient algorithms applied to those studies (which cannot reproduce adequately the polymer dynamics). Once the dynamic procedure starts, the properties of interest are obtained from the polymer unit coordinates every 5 or 10 time units in a range of (5-30) × 10^4 time units (also depending on the system characteristics). The results are stored in arrays to be used for the calculations of different averages over the considered time range, once the simulation trajectory has been completed. These averages are obtained according to the generic formula

$$C(\tau) \equiv \langle C(t,t+\tau)\rangle = 1/(n_t - n_k)\sum_{n_j=1}^{n_t-n_k} C(n_j, n_j+n_k) \quad (1)$$

where $C(n_j,n_j+n_k)$ is evaluated from the values of some property A, stored in the array elements $A(n_j)$ and $A(n_j+n_k)$ which correspond to time units t and $t+\tau$ along the simulation. n_t is the total number of array elements. When A is a property of an individual chain, $C(\tau)$ is also finally averaged over the values of $C(\tau)$ obtained from eq 1 for the different chains of the system.

Calculation of Properties

We have calculated the following averages, related to physical properties:

(a) Equilibrium Averages. We have obtained the quadratic end-to-end distance, $\langle R^2\rangle$, of individual chains with EV in systems with different values of N and Φ, and we have determined the exponent ν, which governs the scaling law $\langle R^2\rangle \sim (N-1)^{\nu}$ for every concentration. The results are not detailed here as they are in complete agreement with previous calculations performed with the MC method that we have used to study equilibrium properties.[16]

(b) The Mean Quadratic Displacement of a Chain. It is defined as

$$C_R(\tau) = \langle[\mathbf{R}_{cm}(t+\tau) - \mathbf{R}_{cm}(t)]^2\rangle \quad (2)$$

where $\mathbf{R}_{cm}(t)$ is the position vector of the center of masses of the chain, which can be easily calculated from the position vectors of the different units, associated to their sites in the configuration, $\mathbf{R}_i$. This property is related to the translational diffusion coefficient, according to the Einstein formula

$$D_t = (1/6\tau)C_R(\tau) \quad (3)$$

(c) Time-correlation functions of the chain of the end-to-end vector ($\mathbf{R}$)

$$\rho_R = \langle \mathbf{R}(t)\cdot\mathbf{R}(t+\tau)\rangle/\langle R^2\rangle \quad (4)$$

and also of first three internal Rouse coordinates ($\mathbf{u}_j$)

$$\rho_j = \langle \mathbf{u}_j(t)\cdot\mathbf{u}_j(t+\tau)\rangle/\langle u_j^2\rangle \quad (5)$$

where

$$\mathbf{u}_j = [(2-\delta_{j0})/N]^{1/2}\sum_{i=1}^{N}\cos[(i-{}^1/_2)\pi j/N](\mathbf{R}_i - \mathbf{R}_1) \quad (6)$$

The Rouse model predicts that,[8] except in the range of very short times, these functions, ρ_R and ρ_j, should obey single exponential decay behaviors, from which one can define the corresponding relaxation times (τ_i)

$$\rho_i(\tau) \sim e^{-\tau/\tau_i} \quad (7)$$

and similar definitions are also employed to describe the dynamics in nondilute regions. (For instance, the reptation theory provides a theoretical description of τ_R.[9])

(d) The Dynamic Form Factor. This is another time-correlation function depending on the coordinates of individual chains

$$S(q,\tau) = (1/N^2)\langle\sum_{j=1}^{N}\sum_{k=1}^{N}\exp\{i\mathbf{q}\cdot[\mathbf{R}_j(t) - \mathbf{R}_k(t+\tau)]\}\rangle \quad (8)$$

where $\mathbf{q}$ is the customarily defined scattering vector. Of course, there is not an imaginary contribution to eq 8, so only the real part is evaluated.

(e) The Dynamic Collective Scattering Function. This property of the system is obtained by taking into account which lattice sites are assigned to polymer units or solvent in the considered configurations. This way, the reduced function is obtained as the real (non-null) component of

$$S_{col}^*(q,\tau) = L^{-3}\langle\sum_{j=1}^{n_s}\sum_{k=1}^{n_s} f_j(t)f_k(t+\tau)\exp\{i\mathbf{q}\cdot[\mathbf{R}_j(t) - \mathbf{R}_k(t+\tau)]\}\rangle \quad (9)$$

where $n_s = L^3$ is the number of lattice sites and the factors $f_i(t)$ are obtained as

$$f_i(t) = 1 - \Phi \quad (10)$$

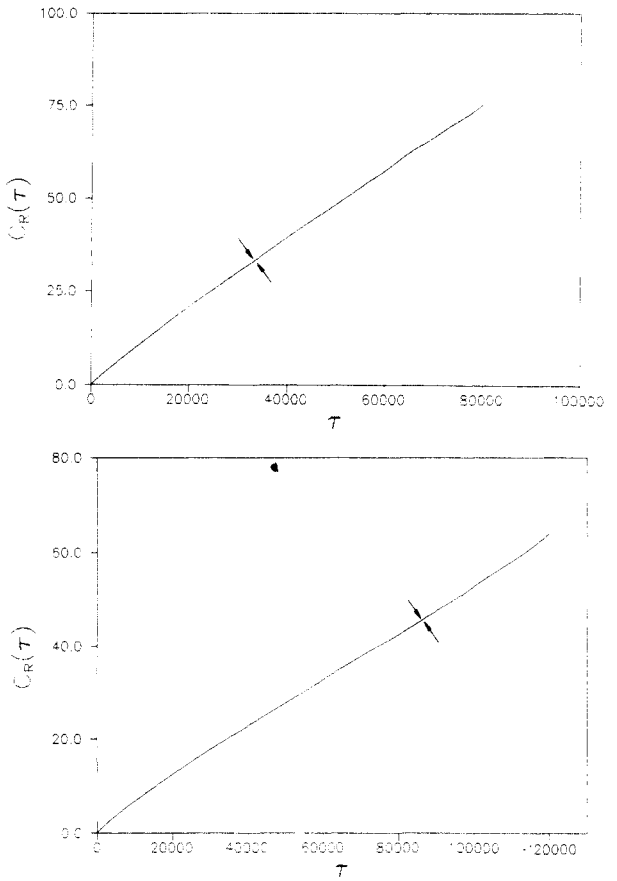

Figure 2. (a) $C_R(\tau)$ (in b^2 units) vs τ (in MC time units) for the $N = 60$ chain at $\Phi = 0.75$. (b) Same plot for the $N = 84$ chain at $\Phi = 0.75$. Arrows indicate the onset of the diffusive regime.

if site i is occupied by a polymer unit at time t, or

$$f_i(t) = -\Phi \tag{11}$$

otherwise. This function is the dynamic equivalent of the equilibrium collective light scattering function that we have used[17] to characterize different properties and evaluate phase separation curves. This scheme is, in fact, equivalent to the previous descriptions of collective scattering functions provided by de Gennes[18] and Binder et al.[19]

We have used several values of q, according to the adequate[17,19] formula

$$q_i = (2\pi/L)k_i \qquad i = x, y, z \qquad k_i = 1, 2, 3, \ldots \tag{12}$$

These values will be denoted in terms of $q^* = qL/2\pi$.

Results and Discussion

Figure 2 shows plots of the results for $C_R(\tau)$ vs τ obtained for several systems. Equation 3 is only valid for times long enough to correspond to the chain diffusive regime. This region is apparently reached[5,7] when $C_R(\tau) > 2\langle S^2\rangle$, where $\langle S^2\rangle$ is the mean quadratic radius of gyration of the chains, average previously evaluated in our study of equilibrium properties.[16] The limit from which this condition is valid is indicated by arrows in Figure 2, and a linear dependence can be appreciate beyond that limit in all cases. (Recent simulations with the bond fluctuation model[20,21] show, however, a decrease of $C_R(\tau)/\tau$ extended to considerably higher times, before the diffusion relaxation time can be reached.) From the slope of our plot in the long time range, it is possible to estimate D_t (in the reduced form consistent with our choices for time and length units). Table I contains a summary of the results

Table I
D_t (in Reduced Units) Obtained from eq 3 for the Different Systems[a]

	$D_t^* \times 10^2$				
Φ	$N = 18$	$N = 36$	$N = 60$	$N = 84$	ν_D
RW	1.57	0.89	0.43	0.35	1.01 ± 0.09
RW-LS	1.54	0.76	0.45	0.36	0.96 ± 0.05
EV	1.38	0.63	0.46	0.29	0.98 ± 0.08
EV-LS	1.72	0.68	0.49	0.30	1.1 ± 0.1
0.195	0.95	0.45	0.34	0.17	1.04 ± 0.15
0.38	0.62	0.26	0.13	0.09	1.27 ± 0.03
0.75	0.09	0.03	0.02	0.01	1.44 ± 0.06

[a] LS denotes results obtained from fits to eq 17.

for different systems. The dependence with chain length for a fixed concentration can be expressed in terms of the exponents ν_D, defined in the scaling law

$$D_t = N^{-\nu_D} \tag{13}$$

and also included in Table I. We have obtained $\nu_D \simeq 1$ in the dilute regime, both for the RW (unperturbed) and the EV (good solvent) models. This is in agreement with the theoretical predictions of the Rouse dynamics[9,10] for a single chain, which models the polymer by means of harmonic springs, ignoring the HI effects between units. The more realistic Rouse–Zimm and Kirkwood–Riseman theories (which incorporate HI in an approximate way) predict $\nu_D \simeq 1/2$ in the absence of EV and $\nu_D \simeq 0.6$ when EV effects are incorporated,[8,9] values much closer to the experimental data. These results are confirmed through Brownian dynamics simulations which include a rigorous description of HI.[22-24] Of course, the commonly employed dynamic MC algorithms (as the one used in the present work) cannot take into account the HI effects. In fact, a more realistic evaluation of D_t for dilute chains with MC methods can be carried out[16] by evaluating the equilibrium reciprocal averages of internal distances between units and introducing these simulation results in the frame of the approximate theories which consider HI.

Then, the main interest of the evaluation of D_t from eq 2 is constituted by the analysis of concentration effects (for nondilute systems the physical importance of HI are greatly diminished as they are screened out). In Table I, we can observe that ν_D increases for increasing values of Φ. ($\nu_D \simeq 1.4$ is obtained for $\Phi = 0.75$, result very close to a previous estimation for a similar volume fraction.[4]) This increase has been also found experimentally.[25,26] The reptation theory yields $\nu_D = 2$ for a entangled system of infinitely long chains. Similar limiting laws can be predicted through different alternative arguments.[7] However, our chains are not long enough to detect the $C_R(\tau) \sim \tau^{1/2}$ intermediate behavior which separates the Rouse and entangled regimes.

In Figure 3, we present an illustration of the results for the different time-correlation functions ρ_R, ρ_1, ρ_2, and ρ_3 (corresponding to $N = 84$, $\Phi = 0.75$). Neglecting the deviation from linearity found at very short times, logarithmic fits allow us to obtain the corresponding relaxation times, τ_i, according to eq 7. The results for relaxation times (expressed in MC time units) are shown in Table II. The results for τ_R and τ_1 are very similar, as it has been also previously reported.[4,27] In Table II, we also present the exponents γ_i, which characterize their variation with chain length for a given concentration, expressed by the scaling law

$$\tau_i \sim N^{\gamma_i} \tag{14}$$

The values of γ_i obtained for dilute chains can be considered in good agreement with those predicted by the

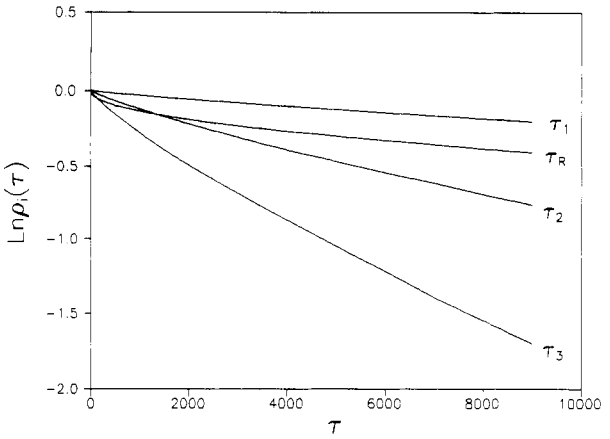

Figure 3. ln $\rho_i(\tau)$ vs τ (in MC units) for the $N = 84$ chain at $\Phi = 0.75$.

Table II
τ_j (in MC Time Units) for the Different Systems

		$\tau_j \times 10^{-2}$				
Φ	j	$N = 18$	$N = 36$	$N = 60$	$N = 84$	γ_j
RW	R	0.4	1.5	4.0	10	2.02 ± 0.09
	1	0.4	1.6	4.4	10	2.06 ● 0.06
	2	0.1	0.4	1.2	2.2	2.02 ● 0.04
	3		0.2	0.5	0.9	1.93 ± 0.06
EV	R	0.8	4.0	11	26	2.20 ± 0.07
	1	0.9	4.1	11	29	2.24 ± 0.10
	2	0.2	1.1	2.7	6.4	2.20 ± 0.10
	3		0.4	1.5	2.7	2.21 ● 0.20
0.195	R	1.2	5.7	19	41	2.312 ± 0.001
	1	1.1	5.7	19	44	2.36 ● 0.02
	2	0.3	1.6	4.5	10	2.31 ● 0.08
	3	0.2	0.7	1.8	4.3	2.15 ± 0.06
0.38	R	1.8	8.9	29	54	2.24 ± 0.06
	1	1.8	9.1	31	60	2.30 ± 0.05
	2	0.4	2.3	7.5	16	2.33 ● 0.02
	3	0.2	1.0	3.3	7.3	2.337 ± 0.008
0.75	R	11	60	18_8	46_3	2.41 ● 0.04
	1	11	63	20_3	50_3	2.46 ± 0.04
	2	2.5	15	48	113	2.45 ● 0.05
	3	1.2	7.1	22	58	2.51 ● 0.08

Table III
Exponent ν_i Obtained from eq 15 for the Different Systems

	ν_i			
Φ	$N = 18$	$N = 36$	$N = 60$	$N = 84$
RW		1.98 ± 0.04	1.94 ± 0.07	2.16 ● 0.02
EV		2.06 ± 0.13	1.84 ± 0.14	2.168 ± 0.009
0.195	1.87 ± 0.13	1.91 ± 0.09	2.12 ± 0.04	2.104 ● 0.002
0.38	2.01 ± 0.03	2.01 ● 0.03	2.036 ± 0.008	1.923 ● 0.005
0.75	2.06 ± 0.05	1.99 ± 0.04	2.04 ± 0.03	1.98 ± 0.14

Rouse theory, $\gamma_i \simeq 2$, for unperturbed (or RW) chains, and $\gamma_i \simeq 2.2$ for EV chains (though the error bars, estimated from simple linear regression analyses, suggest a mean uncertainty of about 0.1 for all these exponents). The increase of γ_i with concentration is similar for all the different exponents (some discrepancies with this uniform behavior have been noticed for the face-centered cubic lattice model[27]). As it is well-known, the reptation theory predicts $\gamma_R = 3$ in the long-chain limit, while experimental results[25] tend to indicate $\gamma_R \simeq 3.4$. Of course, these plateaus cannot be reached for our relatively short chains.

From the results in Table II for τ_1, τ_2, and τ_3, we have also investigated the dependence of τ_i on i, for the different systems, expressed in the form

$$\tau_i \sim i^{-\nu_i} \tag{15}$$

The exponents are contained in Table III (except for the $N = 18$ chain, where τ_3 could not be obtained because it corresponds to a fast motion with a very short decay) and are always close to the value $\nu_i = 2$, expected from the definition of the internal Rouse coordinates (again, a mean uncertainty of about 0.1 can be safely assumed for all these exponents). This seems to indicate that a description of the chain internal motions in terms of the Rouse coordinates is adequate, even in the range of concentrations where the Rouse dynamics cannot be obeyed since the motions are considerably slowed down by interactions with the surrounding chains.

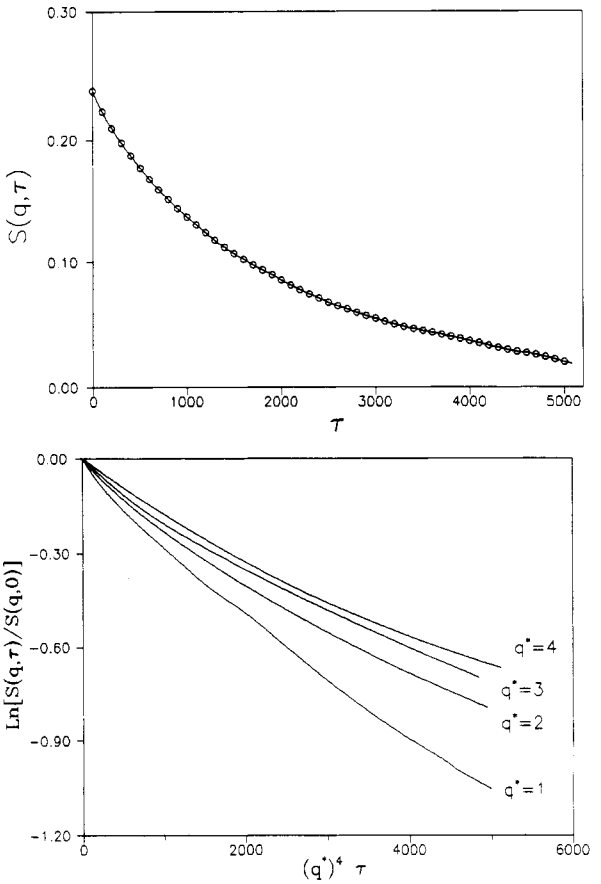

Figure 4. (a) $S(q,\tau)$ vs τ for the $N = 60$ chain, with $q^* = 1$. Solid line: results from eq 8; (O) results from eq 9, single chain, and eq 16. (b) Semilog plot of $S(q,\tau)/S(q,0)$ vs $(q)^4\tau$ for the $N = 84$ chain and different values of q. All the results correspond to the dilute regime.

The dynamic scattering form factor of an individual chain with EV ($N = 60$, $q^* = 1$), obtained from eq 8, is presented in Figure 4a. We also include results corresponding to the dynamic scattering factor for the same single chain dilute system, evaluated from eq 9, since $S(q,\tau)$ and $S_{col}^*(q,\tau)$ are related, according to the expression

$$\lim_{\Phi \to 0} S_{col}^*(q,\tau) = N\Phi S(q,\tau) \tag{16}$$

A complete agreement between both sets of results is observed. These results for dilute system can be able to yield alternative estimation of D_t and some relaxation times. Thus, Pecora obtained the following expression based in the Rouse model:[14]

$$S(q,\tau) = e^{-q^2 D_t \tau}[S_0(x) + S_2 e^{-2\tau/\tau_1} + ...] \tag{17}$$

where the preexponential factors depend on $x \equiv q^2\langle S^2\rangle$. In Table I, we have also included the results for D_t, obtained by fitting the results for $S(q,\tau)$ (calculated with $q^* = 1$) to one exponential, i.e., by neglecting the second and higher terms in the bracket on the right side of eq 17. The results are very similar to those obtained from the study of the displacement of the center of masses, for both RW and

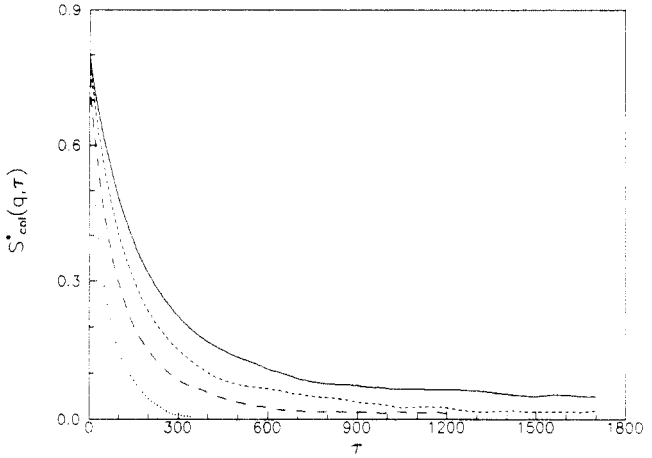

Figure 5. $S_{col}^*(q,\tau)$ vs τ for chains of different number of units at $\Phi = 0.38$, obtained with $q^* = 1$. Solid line, $N = 84$; short dash, $N = 60$; long dash, $N = 36$; points, $N = 18$.

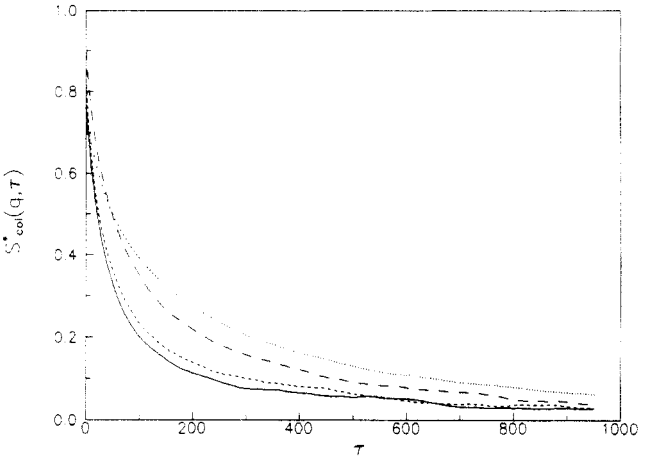

Figure 6. $S_{col}^*(q,\tau)$ vs τ for the $N = 84$ chain at different concentrations with $q^* = 2$. Solid line, $\Phi = 0.38$; short dash, $\Phi = 0.29$; long dash, $\Phi = 0.195$; points, $\Phi = 0.105$.

EV chains (except in the case of $N = 18$, which exhibits a very fast decay for $S(q,\tau)$ due to its small size, for which a precise determination of the fitting parameters is difficult). Then, the Pecora analysis, based in the Rouse model, seems consistent with the dynamics of our MC model in this respect. However, the fitted numerical values for $S_0(x)$ differ significantly from quantitative values derived directly from the Rouse model.[28] A more elaborate fit to the sum of two exponentials has not been able to yield adequate values of τ_1. Of course, a monoexponential behavior is expected for small values of q, according to eq 17.

Although a multiexponential behavior for $S(q,\tau)$ is apparent from the analysis of results obtained with higher values of x (or q^*), the numerical values of the parameters corresponding to the second term do not agree with the values of τ_1 obtained directly from the decay of the Rouse coordinate. Morever, these parameters exhibit some dependence on the time range selected for the fitting procedure, perhaps due to numerical uncertainties. This failure to reproduce the relaxation times contrasts with a previous similar analysis of simulation values of $S(q,\tau)$ calculated for Rouse chains with and without EV in the free space, through the method of Brownian dynamics.[23,24] It is not clear whether the lattice restrictions are mainly responsible for most of the numerical difficulties and physical differences found in the analysis of the present results for single chains.

In Figure 4b, we show a semilog representation of $S(q,\tau)/S(q,0)$ vs $(q^*)^4\tau$ for the $N = 84$, obtained with data calculated for different values of q^* in the dilute regime. The different curves seem to converge to an universal plot as q^* increases, in good agreement with the predictions of the Rouse model[18,24] for intermediate values of q. Recent molecular dynamics simulations for entangled polymer melts[29] show a slowing down at high values of τ in these types of Rouse scaling plots, interpreted as a signature of non-Rouse behavior.

Equation 9 allows also for the calculation of $S_{col}^*(q,\tau)$ in the case of nondilute systems. Previous simulation studies of this property are scarce and devoted only to the very specific case of spinodal decomposition of polymer blends.[30] An illustration of decay curves that we have obtained with $q^* = 1$ for different chains at a fixed concentration ($\Phi = 0.38$) is provided in Figure 5. The longer chains exhibit slower decays, which indicates a residual molecular weight dependence (even at this high concentration) for our relatively short chains. The numerical decay functions have been analyzed by means of the standard DISCRETE routine[31] which is able to fit them to an optimum number of exponential terms. This analysis reveals a clear multiexponential behavior for the results corresponding to most of our different systems. However, the statistical noise precludes meaningful numerical fits to functions including more than two exponentials. Also, recent experimental data[15,32,33] tend to support the presence of several decay contributions, whose amplitudes vary with chain length and solvent quality in a complicate way. Notwithstanding, we have performed preliminary fits to single exponentials, which provide a simple description of the decay curves in the form

$$S_{col}^*(q,\tau) \sim e^{-D_{coop}q^2\tau} \tag{18}$$

where D_{coop} is a cooperative diffusion coefficient which reflects the collective motion of a portion of the system (including several chains) and should not coincide with D_t for nondilute systems. Numerical values of D_{coop} (in reduced units) for the different chain lengths and concentrations, with $q^* = 1$ or 2, are presented in Table IV, where the exponents ν_N and ν_Φ, obtained from fittings to the empirical scaling laws

$$D_{coop} \sim N^{-\nu_N} \tag{19}$$

and

$$D_{coop} \sim \Phi^{\nu_\Phi} \tag{20}$$

are also included. We can observe that, for increasing concentrations, ν_N decreases from the value $\nu_D = \nu_N \simeq 1$,

Table IV
D_{coop} (in Reduced Units) Obtained from eq 18 with Two Values of q, Together with Exponents ν_N and ν_Φ and the Estimated Φ^* for the Different Systems

	$D_{coop}^* \times 10^2$				
Φ	$N = 18$	$N = 36$	$N = 60$	$N = 84$	ν_N
			$q^* = 1$		
0.105	3.6	2.1	1.6	1.4	0.6
0.195	5.3	3.7	3.5	3.0	0.4
0.29	6.8	5.7	5.2	6.0	0.1
0.38	6.5	6.0	5.6	5.4	0.1
ν_Φ	0.5	0.9	1.0	1.1	
			$q^* = 2$		
0.105	3.2	1.6	1.5	1.2	0.6
0.195	3.8	2.8	2.0	1.7	0.5
0.29	4.4	2.8	2.5	2.4	0.4
0.38	4.3	3.2	3.4	2.9	0.2
ν_Φ	0.2	0.5	0.6	0.7	
Φ^*	0.38	0.24	0.16	0.13	

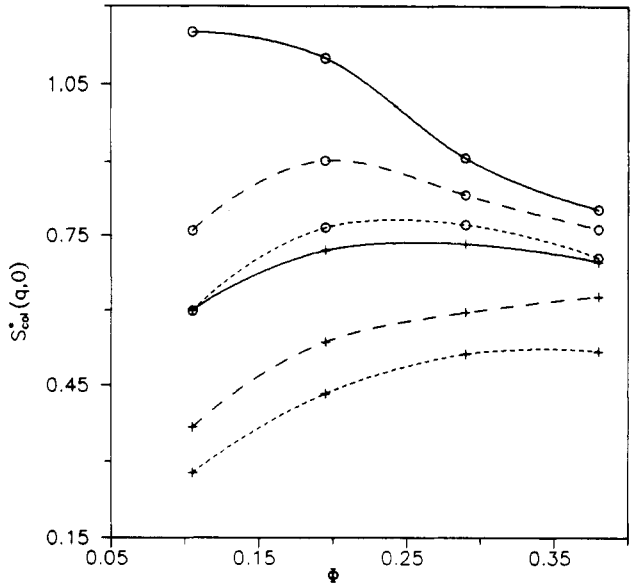

Figure 7. $S_{col}^*(q,0)$ vs Φ for the $N = 18$ (+) and the $N = 84$ (O) chains. Solid line, $q^* = 1$; long dash, $q^* = 2$; short dash, $q^* = 3$.

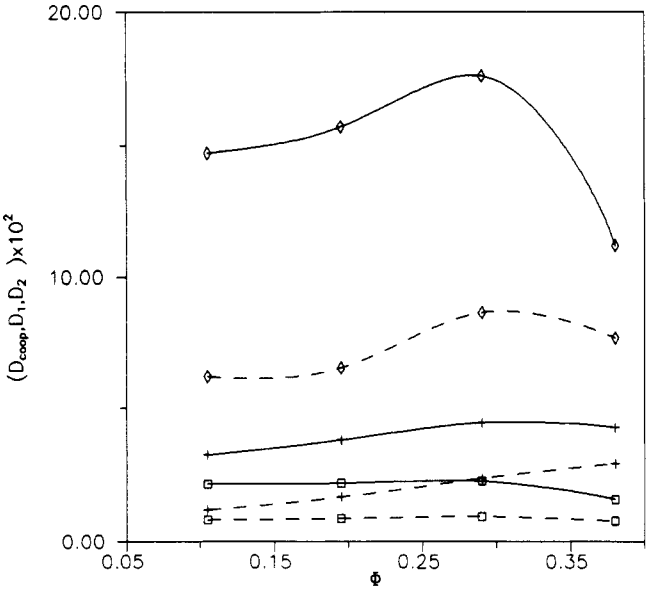

Figure 8. D_{coop} (+), D_1 (□), and D_2 (◇) vs Φ for the $N = 18$ (solid line) and $N = 84$ (dashed line) chains calculated with $q^* = 2$.

obtained in the dilute regime. Of course, the motion monitored by a scattering experiment is less characterized by the length of individual chains in more concentrated systems. The increase of D_{coop} with increasing concentration may seem in contradiction with the decrease in mobility of individual chains for many-chain systems, previously analyzed. However, it has been theoretically explained due to the increase in the restore force of the collective motions. In fact, theoretical estimations[9] and experimental data[15,32,33] support the value $\nu_\Phi \simeq 0.5$–0.75 in semidilute solutions.

The discrepancies in the values of D_{coop} calculated with different q^* represent an additional difficulty in the understanding of these results. As it is well-known, the lower concentration limit of the semidilute region is defined by an overlapping or critical concentration, which can be approximated as $\Phi^* = 3N/4\pi\langle S^2\rangle^{3/2}$, from the values of $\langle S^2\rangle$ previously obtained for the same systems.[16] Typical values of Φ^* for the different chains are included in Table IV. It can be observed that the values of Φ employed in

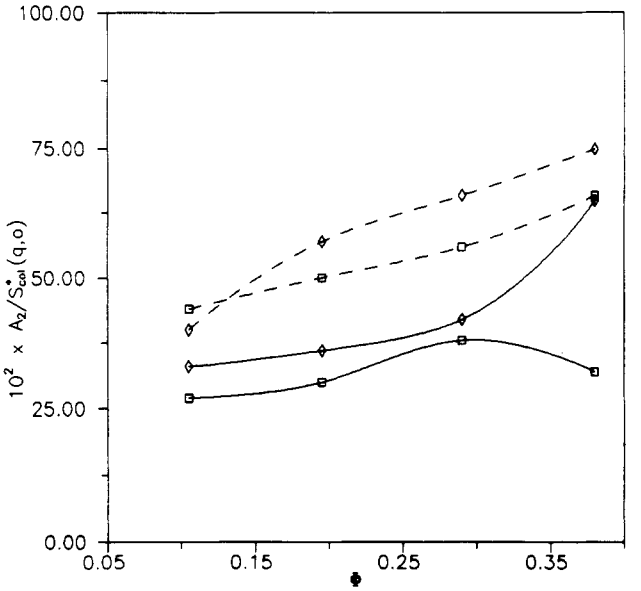

Figure 9. Relative amplitude of the fast mode (2) for the $N = 18$ (□) and the $N = 84$ (◇) chains, with $q^* = 1$ (solid line) and $q^* = 2$ (dashed line).

the simulations are similar or clearly higher than Φ^*, except for the shortest chain, $N = 18$. Moreover, the condition[15,18]

$$(\Phi/\Phi^*)^{-1.125} < q\xi < (\Phi/\Phi^*)^{0.75} \tag{21}$$

can be used to determine the values of q for which eq 20 is valid. ξ is the correlation length corresponding to a diffusive collective fluctuation, so that $D_{coop} = k_B T/6\pi\eta_0\xi$ ($k_B T/6\pi\eta_0$ is the usual combination of the Boltzmann factor and the solvent viscosity in a Stokes–Einstein relationship). On the other hand, the Rouse theory[8] provides the formula $D_t = k_B T/6\pi\eta_0\sigma N$ for the diffusion coefficient of a single Gaussian chain. σ is the Stokes radius of a unit which can be approximately taken[24] as $\sigma/b_{stat} \simeq 0.25$, where b_{stat} is the length of the statistical (Gaussian) segment ($b_{stat} = (^3/_2)^{1/2}b$ for a cubic lattice[8]). Since this result for D_t should be consistent with the values presented in Table I for a random walk, we can estimate the correlation length (in reduced units) as

$$\xi = (^3/_2)^{1/2}(\sigma/b_{stat})ND_t(\mathrm{RW})/D_{coop} \tag{22}$$

This way, and taking into account the lattice lengths adequate[16] for our values of N, in the range $13 \le L \le 23$, we have determined that $q^* = 1$ is too small to monitor properly the collective fluctuations of most systems. However, $q^* = 2$ is more adequate to explore the whole set of systems (except for the shortest chain, $N = 18$). It can be observed that the exponents ν_Φ obtained with $q^* = 2$ and $N > 18$ are fairly consistent with the theoretical and experimental values.

In Figure 6 we have plotted the decay curves obtained for the $N = 84$ chains, with $q^* = 2$ and different values of Φ. The values of $S_{col}(q,\tau)$ are smaller for higher concentrations at long times, due to the faster decays in these systems. However, the values at $\tau = 0$ (which correspond to the static collective scattering) follow a more complicated pattern. As is well-known, and we have verified in previous work,[17] the dependence of the static scattering functions with concentration exhibits a maximum. This is illustrated in Figure 7, where some of our results for the reduced $S_{col}(q,0)$ are presented. This different behavior at short and long times explains the interceptions between some decay curves at intermediate times, observed in Figure 6.

Figure 8 contains the results obtained with the fits of our decay curves for $q^* = 2$ to the sum of two exponentials

$$S_{col}^*(q,\tau) = A_1 e^{-D_1 q^2 \tau} + A_2 e^{-D_2 q^2 \tau} \quad (23)$$

The ratios D_2/D_1 are in the range 5–10, results compatible with the bimodal analysis of experimental data corresponding to flexible chains in good solvents.[15,32] D_2 increases with increasing concentration, though this increase is not maintained for the highest value of Φ.

Figure 9 contains the variation of amplitude for the fast mode, i.e. mode 2, relative to value of the scattering functions at $\tau = 0$ (which should be approximately equal to $A_1 + A_2$). It can be noticed an increase of this mode for higher concentrations and higher values of q. These features are also observed in the analysis of experimental data.[15,32]

Acknowledgment. This work has been supported by Grant PB89-0093 from the DGICYT. A.L.R. also acknowledges a fellowship from the PFPI.

References and Notes

(1) Verdier, P. H.; Stockmayer, W. H. *J. Chem. Phys.* **1962**, *36*, 227.
(2) Baumgartner, A.; Kremer, K.; Binder, K. *Faraday Symp. Chem. Soc.* **1983**, *18*, 37.
(3) Kranbuehl, D. E.; Verdier, P. H. *Macromolecules* **1984**, *17*, 749.
(4) Crabb, C. C.; Kovac, J. *Macromolecules* **1985**, *18*, 1430.
(5) Kolinski, A.; Skolnick, J.; Yaris, R. *J. Chem. Phys.* **1987**, *86*, 7164.
(6) Muller-Krumbhaar, H.; Binder, K. *J. Stat. Phys.* **1973**, *8*, 1.
(7) Skolnick, J.; Kolinski, A. *Adv. Chem. Phys.* **1990**, *78*, 223.
(8) Yamakawa, H. *Modern Theory of Polymer Solutions*; Harper & Row: New York, 1971.
(9) Doi, M.; Edwards, S. F. *The Theory of Polymer Dynamics*; Clarendon Press: Oxford, 1986.
(10) Rouse, P. E. *J. Chem. Phys.* **1953**, *21*, 1272.
(11) Gurler, M. T.; Crabb, C. C.; Dahlin, D. M.; Kovac, J. *Macromolecules* **1983**, *16*, 398.
(12) Kremer, K. *Macromolecules* **1983**, *16*, 1632.
(13) Schaefer, D. W.; Han, C. C. In *Dynamic Light Scattering*; Pecora, R., Ed.; Plenum Press: New York, 1985.
(14) Pecora, R. *J. Chem. Phys.* **1968**, *49*, 1032.
(15) Brown, W. *Macromolecules* **1985**, *18*, 1713.
(16) López Rodriguez, A.; Freire, J. J. *Macromolecules* **1991**, *24*, 3578.
(17) López Rodriguez, A.; Freire, J. J.; Horta, A. Accepted for publication in *J. Phys. Chem.*
(18) de Gennes, P.-G. *Scaling Concepts in Polymer Physics*; Cornell University Press: Ithaca, NY, 1979.
(19) Sariban, A.; Binder, K. *Colloid Polym. Sci.* **1989**, *267*, 469.
(20) Paul, W.; Binder, K.; Herrmann, D. W.; Kremer, K. *J. Phys. II (Paris)* **1991**, *1*, 37.
(21) Paul, W.; Binder, K.; Heermann, D. W.; Kremer, K. *J. Chem. Phys.* **1991**, *95*, 7726.
(22) Fixman, M. *J. Chem. Phys.* **1983**, *78*, 1588.
(23) Rey, A.; Freire, J. J.; Garcia de la Torre, J. *J. Chem. Phys.* **1989**, *90*, 2035.
(24) Rey, A.; Freire, J. J.; Garcia de la Torre, J. *Macromolecules* **1991**, *24*, 4666.
(25) Ferry, J. D. *Viscoelastic Properties of Polymers*; Wiley: New York, 1980.
(26) Graessley, W. W. *Adv. Polym. Sci.* **1982**, *46*, 67.
(27) Crabb, C. C.; Hoffman, D. F.; Dial, M.; Kovac, J. *Macromolecules* **1988**, *21*, 2230.
(28) Perico, A.; Piaggio, P.; Cuniberti, C. *J. Chem. Phys.* **1975**, *62*, 2690.
(29) Kremer, K.; Grest, C. S. *J. Chem. Phys.* **1990**, *92*, 5057.
(30) Sariban, A.; Binder, K. *Polym. Commun.* **1989**, *30*, 205.
(31) Provencher, S. W. *J. Chem. Phys.* **1976**, *64*, 2772.
(32) Brown, W.; Johnsen, R. *Macromolecules* **1986**, *19*, 2002.
(33) Brown, W.; Stepanek, P. *Macromolecules* **1988**, *21*, 1791.